Non-Invasive Dominant Frequency Characterisation of Different Induced Arrhythmias in an Isolated Rabbit Heart Animal Model

Neves Tainan C[1], Quadros Angélica[1], Siles Jimena P[1], Silva Vinicius[1], Sandoval Italo[2], Pachon José Carlos[3], Uzelac Ilija[4], Salinet João[1]

[1] Federal University of ABC (UFABC), São Bernardo do Campo - SP, Brazil
[2] Samsung R&D Institute Brazil (SRBR)
[3] São Paulo Heart Hospital, São Paulo, Brazil
[4] Virginia Commonwealth University, Richmond - Virginia, USA

Abstract

Cardiac diseases are among the main causes of death worldwide. The most used method for evaluating cardiac electrical activity and rhythm is the 12-lead electrocardiogram (ECG), due to its non-invasive nature and easy reproducibility. However, its limited number of electrodes has proven to be a limitation in diagnosing more complex diseases. Results obtained from Body Surface Potential Mapping (BSPM), using a high density of electrodes, allow for the identification of alterations in electrical activity, and this approach overcomes the limitations of the traditional ECG method. In this study, a BSPM system is developed, and its validation is experimentally performed in an in-situ animal model through Lagendorff-isolated rabbit hearts. The non-invasive characterised rhythms were validated through a complex system of multiple simultaneous recordings that involved the non-invasive electric subsystem and a 3 Multi-Electrode Array (MEA) for invasive electrical mapping. Furthermore, the system has a panoramic optical mapping system, the gold standard in electrophysiology, that captures the heart's electrical activity using 3 cameras. This study allowed us to validate a non-invasive electrocardiograph mapping system in an animal model. Establishing frequency parameters for analysing different cardiac rhythms and abnormalities, facing clinical standards for characterising different rhythms.

1. Introduction

Arrhythmia encompasses irregular heart rate and rhythm [1]. The main diagnostic tool is the 12-lead ECG. Cases of supraventricular tachyarrythmias (SVT), such as atrial fibrillation (AF), atrial flutter (AFL) and atrial tachycardia (AT), in 2019, there were over 59.7 million prevalent cases worldwide [2, 3]. Precise SVT diagnosis involves invasive electrophysiology (EP) studies for locating origin sites and mechanisms, often treated by catheter ablation. Despite advances in non-invasive mapping technologies, invasive electrophysiological studies are still crucial for accurate diagnosis and treatment of SVT, as they effectively pinpoint origin sites and mechanisms [4].

Body surface potential mapping (BSPM) can offer high potential for clinical application in low-risk patient settings while providing a wealth of clinical information. It promises to be a low-cost valuable aid in early diagnosis, ablation planning, and post-surgical follow-up [5]. Analysis in dominant frequency (DF) have been used and it seems to find rotational patterns in invasive and non-invasive methodologies.

Identifying the driving mechanisms and their location is crucial to understanding these SVTs and achieving success in ablation therapies, especially for AF patients. Investigators have shown that BSPM allows characterise arrhythmias non-invasively, helping in clinical practice, and decreasing patient exposure to invasive procedures and their associated risks [6]. Additionally, we developed an animal model langendorff perfused rabbit heart experiment of BSPM to study the patterns and electrophysiological maps. Validating it using epicardiac electrical mapping and the optical panoramic electrophysiological map. Thus, in this study, we aimed to evaluate the frequency analysis applied to BSPM signals, epicardial electrograms and optical signals under SVT to validate the BSPM.

2. Material and methods

This study used New Zealand white rabbit (weight of 3.80 ± 0.17 kg) hearts applied into an in-house setup for electrical and optical acquisition of cardiac activity signals. The study was approved by the Ethics Committee on Animal Use (CEUA) at the Federal University of ABC in São Paulo, Brazil, under protocol number 3947230519.

The rabbits were anaesthetised by an intramuscular injection of Buprenorphine (0.05 mg/kg). After 30 minutes, a Ketamine/Xylazine cocktail (150 and 21 mg/kg, respectively) was intramuscularly administered to induce deep anaesthesia. To prevent blood coagulation in coronary veins, Heparin (500 U/Kg) was intravenously infused into the marginal vein of the rabbit's ear. The rabbit hearts were extracted by cutting the upper end of the ascending aorta during a thoracotomy. Before the heart cannulation for reperfusion, it is placed in a reservoir with modified Krebs-Henseleit solution with low calcium concentration (in mM: 115 NaCl, 4.6 KCl, 25 $NaHCO_3$, 0.5 $CaCl_2.2H_2O$, 1.2 KH_2PO_4, 1.2 $MgSO_4.7H_2O$, 1 Na-pyruvate, and 11 glucose $C_6H_{12}O_6$) for blood cleaning and maintainement of heart activity while fat, lung, trachea and connective tissues are removed from the extracted materials.

The heart undergoes retrograde Langendorff perfusion via the aorta using a modified Krebs-Henseleit solution at 37°C. This solution comprises 115 mM NaCl, 4.6 mM KCl, 25 mM NaHCO3, 1.2 mM CaCl2.2H2O, 1.2 mM KH2PO4, 1.2 mM MgSO4.7H2O, 1 mM Na-pyruvate, and 11 mM glucose (C6H12O6). It is continuously bubbled with carbogen gas (5% CO2, 95% O2) to maintain a pH of 7.82±0.09 and a conductivity of 13±1 mS/cm. The perfusion is conducted using a custom-made Langendorff setup, facilitating the circulation of the nutrient solution into the coronary arteries. Once the heart has been established in the Langendorff perfusion system for about 15 minutes, we block the mechanical activity of the heart using (-)-Blebbistatin, avoiding the contraction motion. The procedure involves the perfusion of 75 ml of a modified Krebs-Henseleit solution with 25μM of (-)-Blebbistation, and the use of a modified Krebs-Henseleit solution with 1.7μM of (-)-Blebbistatin throughout the experiment. This procedure is important for optical mapping, as a pixel will represent always the same region in the heart.

A translucent hexagonal tank (18.5x5.5 cm each face) with 60 electrodes (10 per face) was developed for acquiring high-density electrocardiograms for non-invasive mapping. The electrodes are made of stainless steel and are in contact with a sucrose solution (in mM: 23 NaCl, 260 C12H22O11, impedance of 500Ω/cm) circulating within the tank (100 ml/min) at 38°C, simulating trans-thoracic impedance. In the centre of the tank, the heart is placed and perfused retrogradely through the aorta (15-20 ml/min, constant 80 mmHg pressure and 37°C).

Simultaneously, three in-house Multi-Electrode Arrays, each containing 16 silver electrodes, are placed in contact with the epicardiac tissue of the ventricle, left and right atria, for electrical contact mapping. Both epicardial and tank-surface signals are acquired at 4 kHz, amplified at 60 dB, and synchronised (Open Ephys GUI v0.6.6, Open Ephys Acquisition Board v2.4). The reference electrode, made of tinned copper(Cu/Sn), is positioned beneath the aorta on top of the cannula where the heart is fixed for retrograde perfusion. The pre-processing of epicardial signals consisted of applying a Butterworth bandpass filter with a high-pass cutoff (order 20) at 0.5 Hz and a low-pass cutoff (order 10) at 250 Hz. It was followed by a notch filter (order 6, cutoff 60 Hz). Tank signals were filtered using the Discrete Wavelet Transform (DWT) with the Daubechies 4 mother wavelet and 10 decomposition levels. Reconstruction was performed using levels 7 to 10.

A panoramic optical mapping system was applied using 6 deep-red light emission LEDs (650 nm, Luminus Devices) and 3 high-speed cameras (HB-1800-S, Emergent technologies) with C-mount lens (Lens Fujinon CF25ZA, Machine Vision C-Mount / Fujinon) distributed at an angle of 120° to each other and positioned at a fixed distance from the isolated rabbit heart. In this investigation, we introduced 0.2 mg of the voltage-sensitive dye Di-4-ANBDQPQ (Vm, Potentiometric Probes) into the rabbit heart. This incorporation was achieved through multiple perfusion cycles involving 150 ml of a modified Krebs-Henseleit solution, which carried the elution of the dye stock solution (consisting of 0.2 mg of Di-4-ANBDQPQ dye eluted in 200 μL of ethanol). This meticulous process ensures the accurate application of the voltage-sensitive dye for optimal optical mapping results. The 6 LEDs were used to uniformly illuminate the surface of the heart and excite a dye used to highlight the electrical activity of the heart. They were collimated with a condenser lens (ACL2520U-A, Thorlabs) and band-pass filtered (650/40 nm, Thorlabs). Using the Norpix-StreamPix 9 software, we acquired a high-speed 1600x1000 pixels 10 seconds video at 500 frames/s in each camera.

To isolate the atrial signals, the atrioventricular node (AV node) was inhibited from ablating the AV node using a micro-needle linked with a commercial ablation system. Induction of arrhythmia is performed using a custom-made bipolar catheter, combined with the perfusion of a modified Krebs-Henseleit solution containing 1μM of carbachol. The pacing electrode is placed in the left atrium and stimulates the heart to acquire different rhythms.

DF analyses are performed by applying a Hamming window into a 4-second signal for DF calculation, performing zero-padding to enhance frequency resolution, and computing the Fast Fourier Transform (FFT). The resulting spectral data, from all the recorded signals, was denoted and used to estimate the DF within the specified frequency range [7], which may vary depending on the type of rhythm under analysis [7, 8]. DFs were created for each electrode signal and pixels of the images. Visualisation is facilitated through a figure using Laplacian interpolation to display the signals. The DF was calculated by the inverse of the cycle length (CL), where CL is the time, in

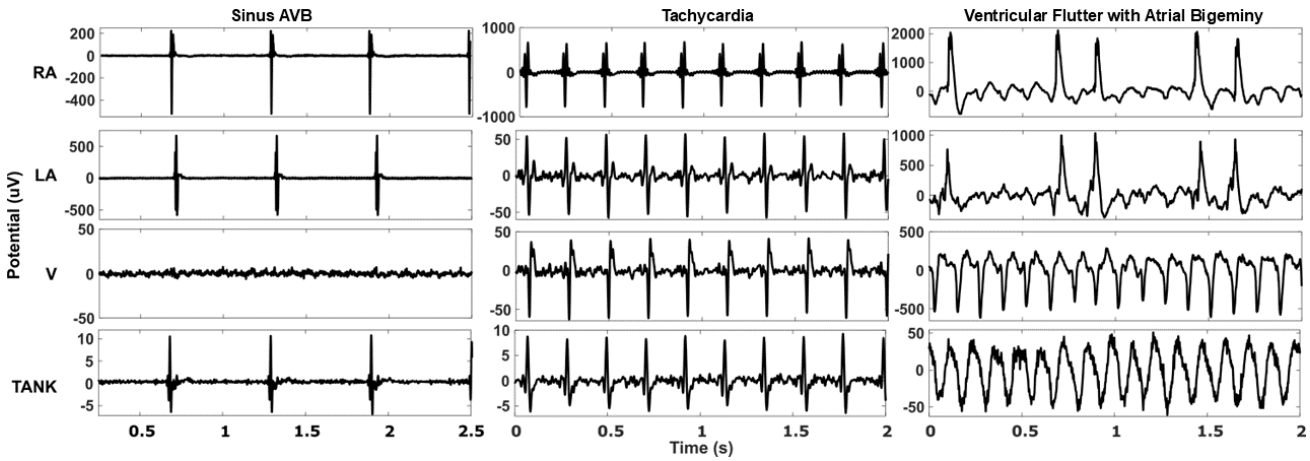

Figure 1. **Cardiac Signals.** Presents optical and epicardial unipolar contact (MEA) signals for right atria (RA), left atria (LA) and ventricle (V), followed by the tank-surface signal. These signals are acquired during a sinus rhythm with atrioventricular node blockage (AVB), tachycardia and Arrhythmia with atrioventricular node dissociation.

seconds, between two consecutive beats. This metric was used as a comparison between the techniques. The Organization Index (OI) is defined as the amount of area, in the analysed frequency spectrum that represents the DF and its harmonics, varying between 0 and 1.

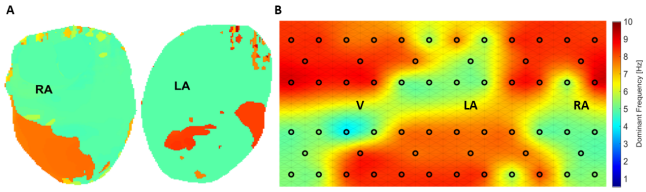

Figure 2. **DF Maps for Optical and non-invasive mapping for ventricular flutter with atrial bigeminy** A – Show an optical DF mapping from RA and LA cameras. B – shows the tank DF map. Black letters indicate the Anatomic reference in the mapping.

3. Results

Fifteen signals were analysed. Figure 1 shows epicardial unipolar contact signals of the right atria, left atria and ventricle respectively, followed by the tank-surface signal. This figure highlights a sinus rhythm with atrioventricular node blockage (AVB), sinus tachycardia and a ventricular flutter with atrial bigeminy. Sinus and tachycardia present uniform activation with constant frequency containing ordinate depolarisation. In the arrhythmic case, the invasive electrical signal delineates specific abnormalities such as ectopic reentrance of atrial depolarisation and ventricular flutter.

To the regular rhythms presented, Table 1 highlights the consistency between DF calculation techniques using the FFT and the inverse of the CL. For regular rhythms, we found a high value of OI. The DF and 1/CL match in values bringing an absolute deviation of less than 0.2 Hz in all cases. In a comparative analysis, we used optical mapping as a reference and highlighted a relative deviation of less than 2% in all cases. Showing that for regular rhythms the tank frequency spectrum reflects the activity in the heart surface.

Figure 2 shows the DF maps in optical (Fig 2A) and tank-surface (Fig 2B) for a ventricular flutter with atrial bigeminy. The rhythm presents two main areas of DF in optical mapping, but they do not divide atria and ventricles. There is a region in the posterior left ventricle with a higher average DF of 7.73$\pm$0.02 Hz and an atrial area with 5.0$\pm$0.7 Hz of average DF. In tank-surface DF mapping, we observe the presence of two different regions, as the optical signal, one with 8.1$\pm$0.4 Hz and 4.9$\pm$0.4 Hz of average DF. The different areas in both methodologies reflect the two different regions in the heart surface.

4. Discussion

The use of a high-density body surface potential mapping (BSPM) system, combined with invasive epicardial electrical mapping and optical panoramic electrophysiological mapping represents a significant advancement in our ability to comprehensively characterise cardiac arrhythmias, experimentally. This integrated approach allows the non-invasive identification of DF patterns and provides an understanding of the underlying mechanisms driving various heart rhythms. The use of three different recording approaches makes the evaluation more robust and allows the validation of standards and parameters for the accurate assessment of cardiac behaviour using the

	Sinus AVB					Tachycardia						
	Optic RA	**Electric RA**	**Optic LA**	**Electric LA**	**TANK**	**Optic RA**	**Electric RA**	**Optic LA**	**Electric LA**	**Optic V**	**Electric V**	**TANK**
DF [Hz]	1.71±0.04	1.72±0.04	1.76±0.04	1.72±0.04	1.74±0.07	4.8±1E-13	4.8±9E-16	4.8±3E-13	4.8±8E-16	4.800±0.008	4.85±0.06	4.80±0.01
OI	0.96±0.02	0.91±0.01	0.96±0.01	0.96±0.01	0.84±0.05	0.96±0.02	0.95±0.02	0.95±0.01	0.92±0.04	0.95±0.01	0.942±0.007	0.962±0.004
1/CL [Hz]	1.650±0.003	1.655±0.004	1.649±0.009	1.650±0.015	1.651±0.002	4.68±0.02	4.63±0.02	4.68±0.01	4.72±0.05	4.68±0.01	4.875±0.008	4.700±0.004
Abs De [Hz]	0.06±0.01	0.06±0.01	0.10±0.01	0.07±0.01	0.09±0.01	0.12±0.01	0.17±0.01	0.12±0.01	0.08±0.01	0.12±0.01	0.026±0.01	0.101±0.01
Comparative Analysis	**RA / MEA**	**RA / TANK**	**LA / MEA**	**LA / TANK**		**RA / MEA**	**RA / TANK**	**LA / MEA**	**LA / TANK**	**V / MEA**	**V / TANK**	
DF$_{RD}$ [%]	0.46±0.01	1.5±0.07	1.9±0.06	1.2±0.06		0	0.012	0	0.012	1.019±0.01	0	
1/CL$_{RD}$ [%]	0.34±0.008	0.2±0.02	0.03±0.0005	0.1±0.04		1.23±0.03	1.53±0.03	0.793±0.04	0.358±0.005	3.94±0.06	0.300±0.005	

Table 1. **DF for regular rhythms.** Data collected from a sinus rhythm with AV node blockage, showing only atrial activations, and sinus tachycardia. The table highlights the values of average DF, OI, and 1/CL, along with the absolute deviation between the two techniques of DF calculation. In the comparative analysis, we observed a relative deviation between the optical analysis (taken as a reference) and the MEAs and tank-surface electrodes in each anatomic reference. De refers to Deviation, and $_{RD}$ is the relative deviation.

torso-tank model.

Optical, epicardial, and tank-surface electrical signals provide valuable insights into cardiac dynamics, with each method offering unique strengths. Invasive signals capture detailed arrhythmic abnormalities, while non-invasive methods reflect cardiac activity but lack anatomical references, limiting the association of BSPM potentials with specific heart regions. Combining these approaches we can enhance our understanding of cardiac activity and support the development of this animal model for non-invasive BSPM mapping animal model. Our results show a low relative deviation when comparing tank-surface electrodes with optical and epicardial signals, validating our setup for regular rhythms. The setup also holds promise for characterising irregular rhythms, although anatomical references in tank-surface signals still need refinement.

The promising results from DF analysis pave the way for further exploration of additional electrophysiological parameters. Future research will integrate complementary analyses to gain deeper insights into cardiac electrical activity, understand arrhythmia mechanisms, and support translational research for clinical implementation.

Acknowledgments

This study is supported by grant no. 2018/25606-2, São Paulo Research foundation (FAPESP) and CNPq INCT INTERAS. call 58/2022. Neves, Tainan was supported by Coordenacão de Aperfeiçoamento de Pessoal de Nível Superior – Brasil (CAPES) and is supported by FAPESP grant #2024/02521-2. J.G. Siles-Paredes and Angélica Quadros are supported by FAPESP grants #2020/03601-9 and #2023/06306-6, respectively.

References

[1] Duncan K, Al-Haddad M. Arrhythmias. Lessons from the ICU 6 2023;185–194. ISSN 25225936.

[2] Page RL, Joglar JA, Caldwell MA, Calkins H, Conti JB, Deal BJ, Estes NA, Field ME, Goldberger ZD, Hammill SC, Indik JH, Lindsay BD, Olshansky B, Russo AM, Shen WK, Tracy CM, Al-Khatib SM. 2015 acc/aha/hrs guideline for the management of adult patients with supraventricular tachycardia: Executive summary: A report of the american college of cardiology/american heart association task force on clinical practice guidelines and the heart rhythm society, 4 2016.

[3] Bollmann A, Lombardi F. Electrocardiology of atrial fibrillation: Current knowledge and future challenges. IEEE Engineering in Medicine and Biology Magazine 2006;25:15–23. ISSN 07395175.

[4] Wellens HJ, Brugada P. Mechanisms of supraventricular tachycardia. The American Journal of Cardiology 1988; 62(6):10–15. ISSN 0002-9149.

[5] Guillem MS, Climent AM, Millet J, Ángel Arenal, Fernández-Avilés F, Jalife J, Atienza F, Berenfeld O. Noninvasive localization of maximal frequency sites of atrial fibrillation by body surface potential mapping. Circulation Arrhythmia and Electrophysiology 2013;6(2):294–301.

[6] Yamashita S, Shah AJ, Mahida S, Sellal JM, Berte B, Hooks D, Frontera A, Jefairi NA, Wielandts JY, Lim HS, Amraoui S, Denis A, Derval N, Sacher F, Cochet H, Hocini M, Jaïs P, Haissaguerre M. Body surface mapping to guide atrial fibrillation ablation. Arrhythmia Electrophysiology Review 201543172–6 2015;.

[7] Salinet JL, Tuan JH, Sandilands AJ, Stafford PJ, Schlindwein FS, Ng GA. Distinctive patterns of dominant frequency trajectory behavior in drug-refractory persistent atrial fibrillation: preliminary characterization of spatiotemporal instability. Journal of cardiovascular electrophysiology 2014;25:371–379. ISSN 1540-8167. URL https://pubmed.ncbi.nlm.nih.gov/24806529/.

[8] Salinet JL, Oliveira GN, Vanheusden FJ, Comba JLD, Ng GA, Schlindwein FS. Visualizing intracardiac atrial fibrillation electrograms using spectral analysis. Computing in Science and Engineering 2013;15:79–87. ISSN 15219615.

Address for correspondence:

Tainan Cerqueira Neves
Alameda da Universidade, S/N. Lab 107, Block Zeta.
São Bernardo do Campo - SP
Brazil
tainan.neves@ufabc.edu.br